Research on Engineering Structures & Materials
www.jresm.org
Research Group

Research Article

Enhancing the performance of cold bitumen emulsion mixtures with coir and glass fibres: Experimental and numerical analysis

Fatimah Fahem Al-Khafaji *,a

Environmental Engineering Dept., Faculty of Engineering, University of Babylon, Babylon, Iraq

Article Info

Article History:

Received 27 Mar 2025

Accepted 25 June 2025

Keywords:

Cold bitumen emulsion mixtures;
Hot mix asphalt;
Natural waste coir fibres;
Synthetic glass fibres;
Finite element analysis;
ABAQUS

Abstract

Cold bitumen emulsion mixtures (CBEMs) offer significant benefits over hot mix asphalt (HMA), including sustainable energy consumption, eco-friendliness, and cost-effectiveness. However, their adoption is limited due to prolonged curing times and low early-life strength. This study examines the reinforcing process of CBEMs with both coir fibres as eco-friendly waste additives and glass fibres as synthetic additive to enhance crack resistance and prolong pavement life. The developed CBEMs are evaluated in terms of tensile strength, creep behavior, fracture toughness, and rutting resistance, using an optimal fibre length of 15 mm and a content of 0.4% by the aggregate weight. Employing both coir and glass fibre reinforcement within CBEMs led to increase the tensile strength by 47% and 87%, respectively. Creep strain was reduced by 33.3% and 56.7% at 60° C after 4000 seconds, while at 40° C, the reductions reached 10% and 66.7%. Fracture toughness increased by 52% and 85%, and rutting depth decreased by 43% and 56%, respectively. The best results were achieved by the glass fibre-reinforced CBEM, which exhibited the highest structural performance, durability, and moisture resistance. The implemented finite element modelling (FEM) using ABAQUS software strongly aligns with experimental results in terms of performance behavior. The adopted statistical analysis confirmed considerable alignment between experimental and numerical results regarding fracture toughness and crack length, thereby validating the reliability and accuracy of the FEM approach.

1. Introduction

1.1 Research Background

CBEMs have proven to be an efficient substitute for conventional HMA, as their production requires less energy due to processing at lower temperatures [1]. CBEMs produce fewer emissions while consuming less fuel, thereby contributing to cost reduction [2]. The longer curing time and initial weakness in such mixtures limited their large-scale application in road paving projects. In order to address these matters, some new researches have tried to enhance the mechanical properties of CBEMs by adding reinforcing material in the form of coir fibres (natural additives) and glass fibres (synthetic additives) [3]. Coir fibers are actually obtained from coconut husk (one of the residues from agriculture) and glass fibers are generated from silica glass with excellent strength in addition to light weight [4]. The incorporation of these reinforcements greatly improves the tensile strength, rutting resistance, stiffness, and cracking resistance of CBEMs, providing a more effective alternative to conventional HMA.

*Corresponding author: mat.fatimah.fahem@uobabylon.edu.iq
[a]orcid.org/0009-0004-3050-846X
DOI: http://dx.doi.org/10.17515/resm2025-786ma0327rs

The semi-circular bending (SCB) test has emerged as a reliable method for assessing the fracture characteristics of asphalt mixtures offering valuable insights into how cracks develop and propagate under load [5]. In addition, indirect tensile stiffness modulus (ITSM) test, creep test, and Hamburg wheel-track test (HWTT) are commonly used to evaluate the performance of CBEMs. Finite Element Modeling (FEM) in pavement engineering enables a comprehensive evaluation of material responses under diverse loading scenarios [6]. The extended finite element method (XFEM), in particular, excels at simulating crack propagation without the need for remeshing, making it a valuable technique for assessing the performance of fiber-reinforced materials [7]. A statistical approach has been included in this study to confirm the alignment between the experimental and numerical results.

1.2 Literature Review

The literature on CBEMs highlights several studies that have explored various methods for improving their performance. Wu S et al. [8], reviewed various fibres in asphalt pavements, highlighting their performance and test methods. Basalt, polyester, cellulose, steel, glass, lignin, and polypropylene fibres were found to improve properties such as rutting resistance, tensile strength, fatigue life, and moisture resistance, with tests like Marshall stability, indirect tensile strength, and fatigue life tests used for evaluation. This summary provided a foundation for identifying the novelty of the current study. Solak H et al. [9] examined the use of synthetic fibers in asphalt pavements, highlighting improvements in tensile strength, fatigue resistance, rutting, and moisture damage. The study summarized the effectiveness of polypropylene and polyester fibers and presented common evaluation methods, including the Marshall stability test, indirect tensile strength test, and wheel tracking test. This review provided a clear foundation for optimizing fiber-reinforced asphalt mixtures. Addae DT et al. [10] conducted a comprehensive review of cold mix asphalt (CMA) mixtures, examining the effects of modifiers, curing conditions, and compaction methods on their mechanical, functional, and long-term performance. The study highlighted improvements in stiffness, rutting resistance, moisture susceptibility, and aging durability, providing a foundation for developing sustainable and durable CMA mixtures. Jain S et al. [11] provided an overview of CMA technology, discussing its materials, design procedures, field applications, and performance characteristics. They emphasized CMA's cost-effectiveness, lower energy consumption, and environmental benefits compared to hot mix asphalt. The study also addressed challenges such as lower early strength and longer curing times, highlighting the need for further research to enhance CMA's mechanical properties and broaden its applications.

Guo Q et al. [12] explored the effects of various fibres, including glass, basalt, and steel, on asphalt mixtures, specifically their impact on low-temperature properties and cracking resistance. The study reveals that fibre-reinforced asphalt concrete (FRAC) demonstrates greater fracture energy (FE) and dissipated creep strain energy (DCSE) than the control concrete. This research contributed to the development of more durable asphalt pavements in cold climates.

Li Z et al. [13] analyzed the characteristics of bagasse fibers and their impact on asphalt mixtures. The study focused on surface modifications to improve fiber compatibility with asphalt, enhancing high-temperature deformation resistance and water stability, though slightly reducing low-temperature performance. The findings suggested that with proper treatment, bagasse fibers could effectively reinforce asphalt pavements. In addition, Malik et al. [14], carried out a laboratory-driven investigation into the performance of CBEMs incorporating waste glass as a partial replacement for fine aggregates. The study aimed to evaluate the mechanical properties and durability of these modified mixtures. Key findings indicated that the inclusion of waste glass enhanced the stiffness and rutting resistance of the CBEMs, while maintaining acceptable levels of moisture susceptibility. These results suggest that utilizing waste glass in CBEMs can be a sustainable approach to improving pavement performance while addressing environmental concerns related to glass waste disposal. Moreover, Briceño-Balza et al. [15], performed a study on the indirect tensile strength and stability of fiber-reinforced cold asphalt mixes, incorporating synthetic microfibers. The results showed that adding 0.05% and 0.10% microfiber slightly weakened the mixtures, while 0.15% improved performance.

The study, prepared by Hubbard-field method with ITS tests, revealed the potential of microfibers to improve the properties of cold asphalt. Overall, the literature underscores the potential of fibre-reinforced CBEMs as a sustainable alternative to HMA, with FEM providing a robust framework for analyzing and predicting their performance under real-world conditions.

1.3 Research Novelty

The novelty of this study is to exploit natural and synthetic fibres to improve the mechanical properties of cold asphalt mix in terms of crack resistance, tensile strength, rutting and creep resistance. The integration of FEM in ABAQUS to simulate fibre reinforcement effects is a novel approach, offering a detailed understanding of material performance and validating the superior performance of the adopted fibres through both experimental and numerical methods. Conducting a statistical analysis to confirm the alignment between the experimental and the conducted FAM results in terms of efficiency and structural integrity.

1.4 Research Main Objectives

- To investigate the influence of natural and synthetic fibres in boosting the crack resistance, tensile strength, rutting and creep resistance of cold asphalt mixture.
- To use of FEA with ABAQUS to simulate the effects of fibre reinforcement on CMA.
- To compare the performance of different fibres, identifying the most effective reinforcement method for enhancing the longevity and durability of pavements.
- To confirm the alignment between the experimental and the simulated FAM results using statistical approach.

2. Materials and Testing

2.1 Materials

The research focused on selecting a suitable cold bituminous emulsion mixture (CBEM) based on material availability and full-scale testing. Crushed granite was used as the aggregate, with its gradation and physical properties detailed in Tables (1) and (2). The aggregates were prepared in accordance with BS EN 933-1 standards [16]. A cationic slow-setting bituminous emulsion (C50B3) with a 40-60 penetration grade was chosen for its strong bonding properties. Limestone dust, comprising approximately 6% of the aggregate's weight, was used as a filler. The used additives are selected from two origins as follow:

- Coir fibres, as natural additives, are extracted from the husk of coconuts, which are considered waste materials, as shown in Figure (1). Their utilization not only reduces environmental waste but also promotes sustainable resource management by repurposing discarded materials. They are strong, durable, and biodegradable, making them an eco-friendly material [17].
- Glass fibres, as synthetic additives, are thin, strong, and lightweight fibres made from silica-based glass as shown in Figure (2), commonly used as reinforcement in composite materials [18]. They are produced by melting glass and drawing it into fine strands, offering high strength, durability, and resistance to heat and chemicals.

Table 1. Maximum aggregate size of 14 mm [19]

Size of the sieve (mm)	14	10	6.3	2	1	0.063
Passing precents (standard limits)	100	77 – 83	52 – 58	25 – 31	14 – 26	6
Passing precents (approved gradation)	100	80	55	28	20	6

Table 2. Physical properties of aggregate

Physical properties	Coarse Agg.	Fine Agg.
Bulk density by (g/cm^3) [20]	2.87	2.76
Apparent density by (g/cm^3) [20]	2.93	2.83
Water absorption by (%) [20]	0.7	1.6

Fig. 1. Coir fibres

Fig. 2. Glass fibres

2.2 Optimization of Fibres as Reinforcement Material

Glass fibers were selected to optimize and enhance the stiffness of CBEM. Laboratory tests assessed the effects of different fiber lengths (10 mm, 15 mm, and 20 mm) and contents (0.3%, 0.4%, and 0.5% of the aggregate's total weight). The results identified the optimal fiber content and length as 0.4% and 15 mm, respectively, as shown in Figure (3). For the record, the same optimum fibre content and length were adopted for the coir fibres on order to conduct a suitable comparison between both additives within CBEMs, acknowledging that their effectiveness differ due to the distinct properties for each fibre type. The addition of coir and glass fibres to CBEMs can reduce workability by increasing internal friction and viscosity, affecting mixing and construction feasibility. Although, the conducted dosage of fiber content for both types was selected at 0.4% by weight of aggregate as the optimum dosage based on multiple trials to ensure a balanced blend. This level provided improved mechanical performance with minimal impact on workability and compaction, maintaining practical constructability for both coir and glass fibre-reinforced CBEMs.

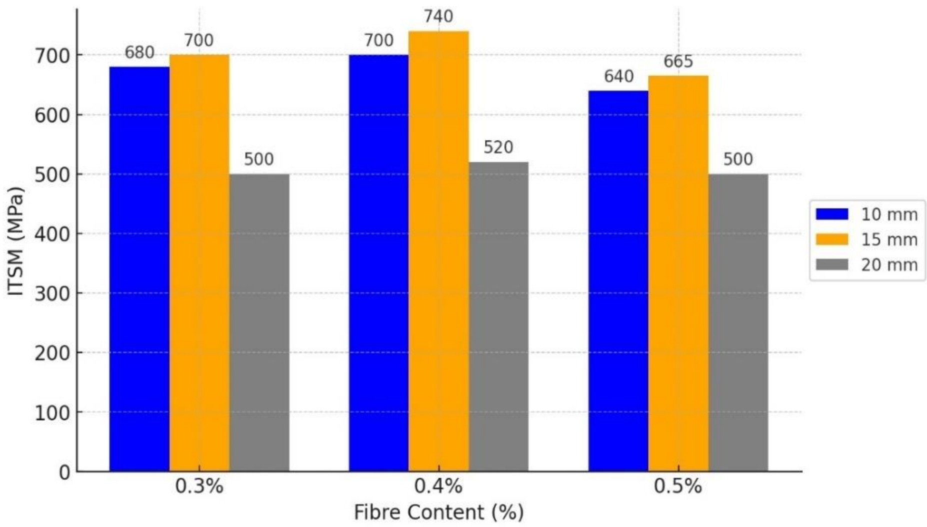

Fig. 3. Optimization of glass fibres

2.3 Mix Design

The Cold bitumen emulsion mixtures (CBEM) mix design was developed following the Asphalt Institute's MS-14 methodology [21], incorporating pre-mixing water contents ranging from 3% to 6% by aggregate mass. Using equations (1) and (2), the Initial Emulsion Content (IEC) was calculated as 6.16%. After several trials, it was conducted that a 3% pre-moisture content ensured proper coverage for CBEM preparation.

$$P = 0.7 \times (0.5C + 0.05A + 0.1B) \tag{1}$$

Where: P: Initial content of the bituminous residual (% of total dry weight of aggregate); C: The passed weight of aggregate from sieve 0.075 mm; A: The retained weight of aggregate on sieve 2.36 mm; B: The retained weight of aggregate on sieve 0.075 mm and passed sieve 2.36 mm.

$$I.E.C = \frac{P}{X} \tag{2}$$

Where: *I.E.C*: Initial emulsion content (% of total mixture mass); X: Bituminous emulsion content. The calculated initial emulsion content was 12.35% of aggregate weight. CBEM samples were prepared using a mixer as in Figure (4), combining water, filler and aggregate for 1 minute at low rapidity. The emulation of bitumen was gradually introduced after 30 seconds, while mixing was maintained for an additional 1.5 minutes.

Fig. 4. Mixer machine

2.4 Testing Procedures

After determining the optimal mixtures, the next step was studying the importance of crack propagation on the engineering and material characteristics of CBEMs for the cold course of surface. This was achieved via a sequence of experimental tests, including indirect tensile stiffness modulus test (ITSM), semi-circular bending test (SCB), and creep test. These assessments measured the modules of stiffness and the ability of CMA to resist propagation of crack.

2.4.1 Crack Propagation Test (Semi-Circular Bending - SCB)

The fracture toughness or tensile strength of bituminous mixtures was measured using the bending test (SCB), following BS EN 12697-44 [22]. CBEM mixtures, prepared as described in section 2.3, were compacted into half-cylinder specimens measuring 150 mm in diameter and 50 mm in thickness. A notch, 2 mm in wide and 10 mm in deep, was made at the center of each specimen to evaluate crack growth, in accordance with the standard [23], as shown in Figure (5).

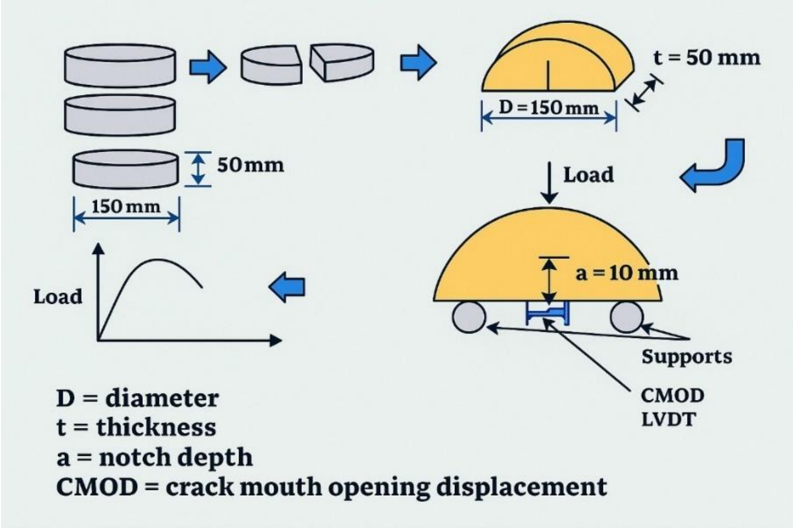

Fig. 5. The diagram of semi-circle bending samples preparation and test procedure

The bottom of each semi-circular sample experienced tensile stress by applying a load from the top with a three-point bending system at 5° C, as illustrated in Figure (5). In accordance with BS EN 12697-44 [22], the test was performed at a constant deformation rate of 5 mm/min, gradually increasing the load until the maximum force (F max) was achieved. This force is directly related to the specimen's resistance to crack propagation (fracture toughness). Figures (6) and (7) illustrate a demonstration of semi-circle bending evaluation. Through the test, the maximum load prior to the failure being recorded [23]. By means of BS EN 12697-44 [22], the concentrated stress at failure (σ_{max}) and toughness of fracture (Kic) were considered using the following equations:

$$\sigma_{max} = \frac{4.263 \times F_{max}}{D \times t^2} \tag{3}$$

Where: *D*: Specimen diameter by (mm); *t*: Specimen thickness by (mm); *F max*: Maximum force by (N); *σ max*: Maximum level of stress at failure by (N/mm^2).

$$Kic = \sigma_{max} \times f\left(\frac{a}{w}\right) \tag{4}$$

Where: *W*: Specimen height by (mm); *A*: Specimen notch depth by (mm); *σ max*: Maximum stress at failure by (N/mm^2); *f (a/W)*: Specimen geometric factor = 5.956 at 9 < a < 11 (mm) and 70 < W < 75 (mm).

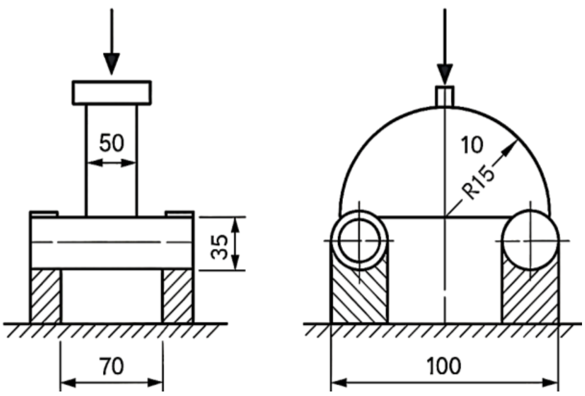

Fig. 6. The specimen of semi- circle plan

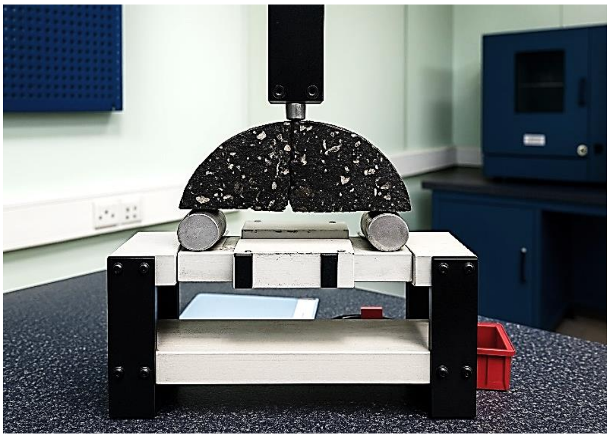

Fig. 7. The semi-circle specimens in laboratory

2.4.2 Indirect Tensile Stiffness Modulus (ITSM) Test

The ITSM test, conducted in accordance with BS EN 12697-26 [24], evaluates the stiffness modulus of cold mix asphalt (CMA) samples under varying curing times and temperatures. This test operates by applying a repeated compressive load along the vertical diametrical plane of a cylindrical specimen, generating indirect tensile stress within the material. The corresponding horizontal deformation is measured to determine the stiffness modulus, which represents the asphalt mixture's ability to resist deformation under loading conditions. Figure (8) illustrates the ITSM testing apparatus.

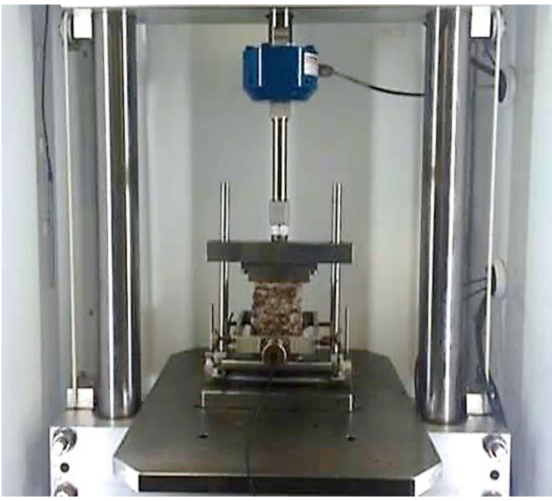

Fig. 8. Apparatus for indirect tensile test

2.4.3 Creep Test

The test of creep, focused in conformity of BS EN 12697-25 [25], evaluated the viscoelastic properties of CBEMs under sustained loading, comparing reinforced and unreinforced samples. In this test, a static load is exerted on a cylindrical asphalt sample at a specified temperature for a defined period. The resulting time-dependent deformation (creep) is measured to evaluate the mixture's ability to resist rutting and long-lasting deformation under continuous traffic loads [25]. Figure (9), depicts the creep test configuration.

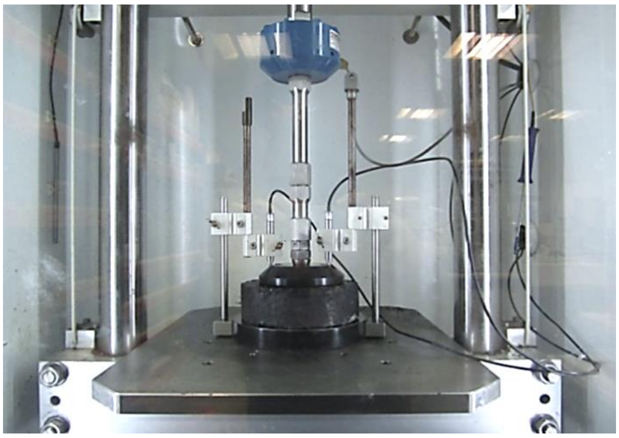

Fig. 9. Creep test configuration

2.4.4 Humburg Wheel Track Test

The HWTT, which is described by EN 12697-22 [26], is European standard to assess rutting resistance and moisture susceptibility of asphalt mixes under simulated traffic loading. A standard load of 705 ± 10 N is applied by a steel or rubber wheel that applies repeatedly over the surface of the sample, which is brought to raised temperature (usually 50° C) and positioned underwater as shown below in Figure (10). The test measures rut depth over time and runs for a maximum of 20,000-wheel repetitions or when a target rut depth is achieved, and gives insight into how resistant an asphalt mixture is to permanent deformation and moisture damage, especially for surface courses under climatically sensitive conditions. Test samples prepared for the Hamburg wheel-track test are normally about 320 mm long, 260 mm wide, and 60 mm thick, as presented in Figure (11). These slabs are compacted within a specified mold by using a lab pneumatic roller compactor, as shown in Figure (12) according to EN 12697-33 and ASTM D8079 [26].

Fig. 10. The apparatus of Hamburg wheel-track

Fig. 11. Hamburg wheel-track sample

Fig. 12. Lab pneumatic roller compactor

3. Finite Element Modelling FEM

Finite element analysis in ABAQUS involved splitting the model to tiny elements, which were linked by shared nodes. The integrating of elements and nodes created a mesh, with mesh density determined by the number of elements. Loads and boundary conditions were applied to the nodes, and stress analysis was performed to assess strain, displacement and stresses in every component [27]. The extended finite element analysis (XFEA) was used for crack growth modeling, differing from conventional FEM by introducing special displacement functions based on the partition of unity theory. This approach prevents discontinuities within elements and allows crack growth simulation without remeshing [27].

The fracture progression in the SCB test was analyzed using XFEM, as illustrated in Figure (13), which depicts crack growth prediction for a CBEM specimen with a 10 mm notch depth. Additionally, Figure (14), presents the maximum load and displacement of a typical cold mix asphalt sample at 97 second of step time, which is the best period for evaluating the material's performance. In addition, ABAQUS software was used to simulate the experimental rut behavior, enabling accurate prediction of rut depth progression under repeated loading.

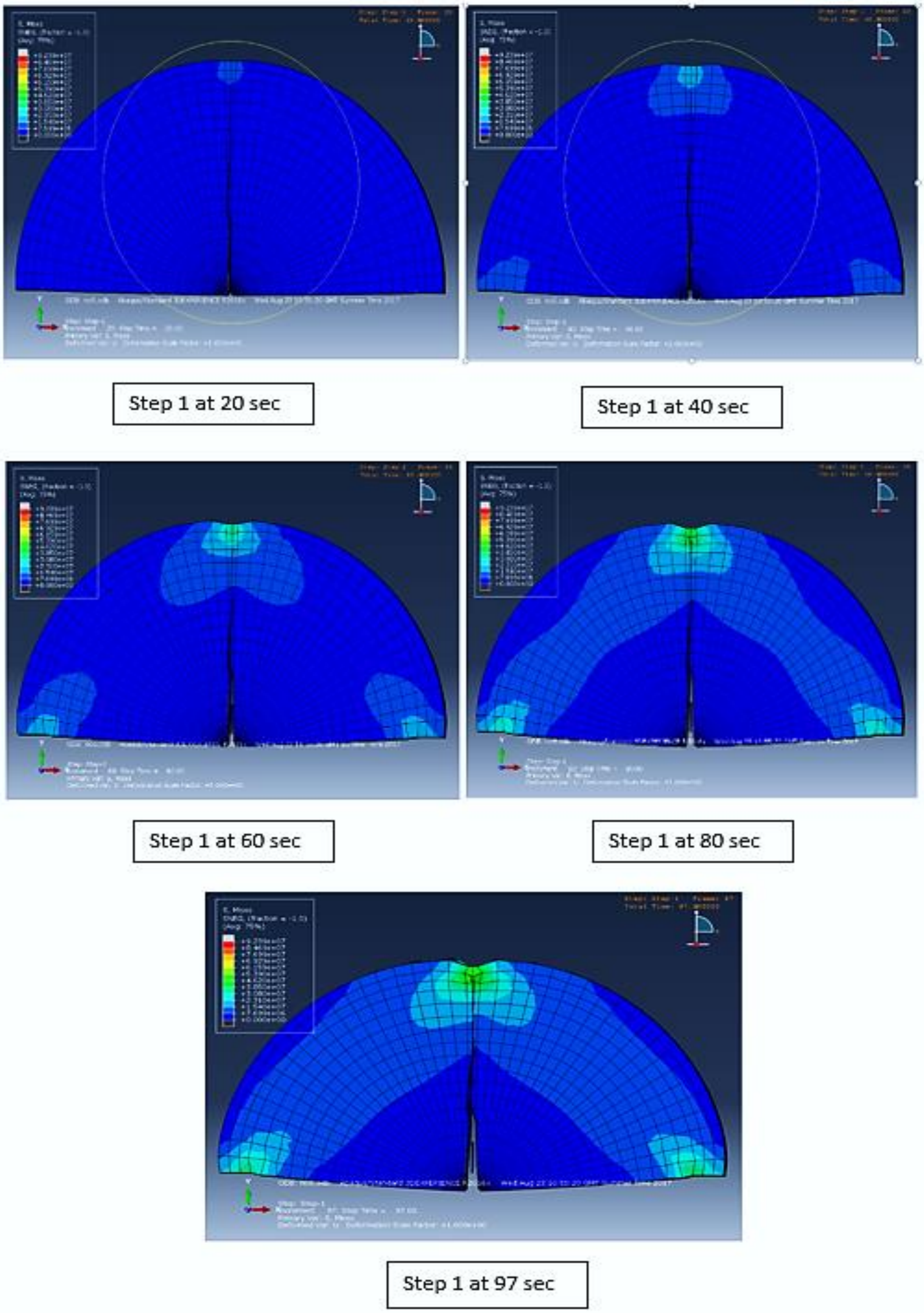

Fig. 13. Propagation of crack for conventional semi-circle specimen

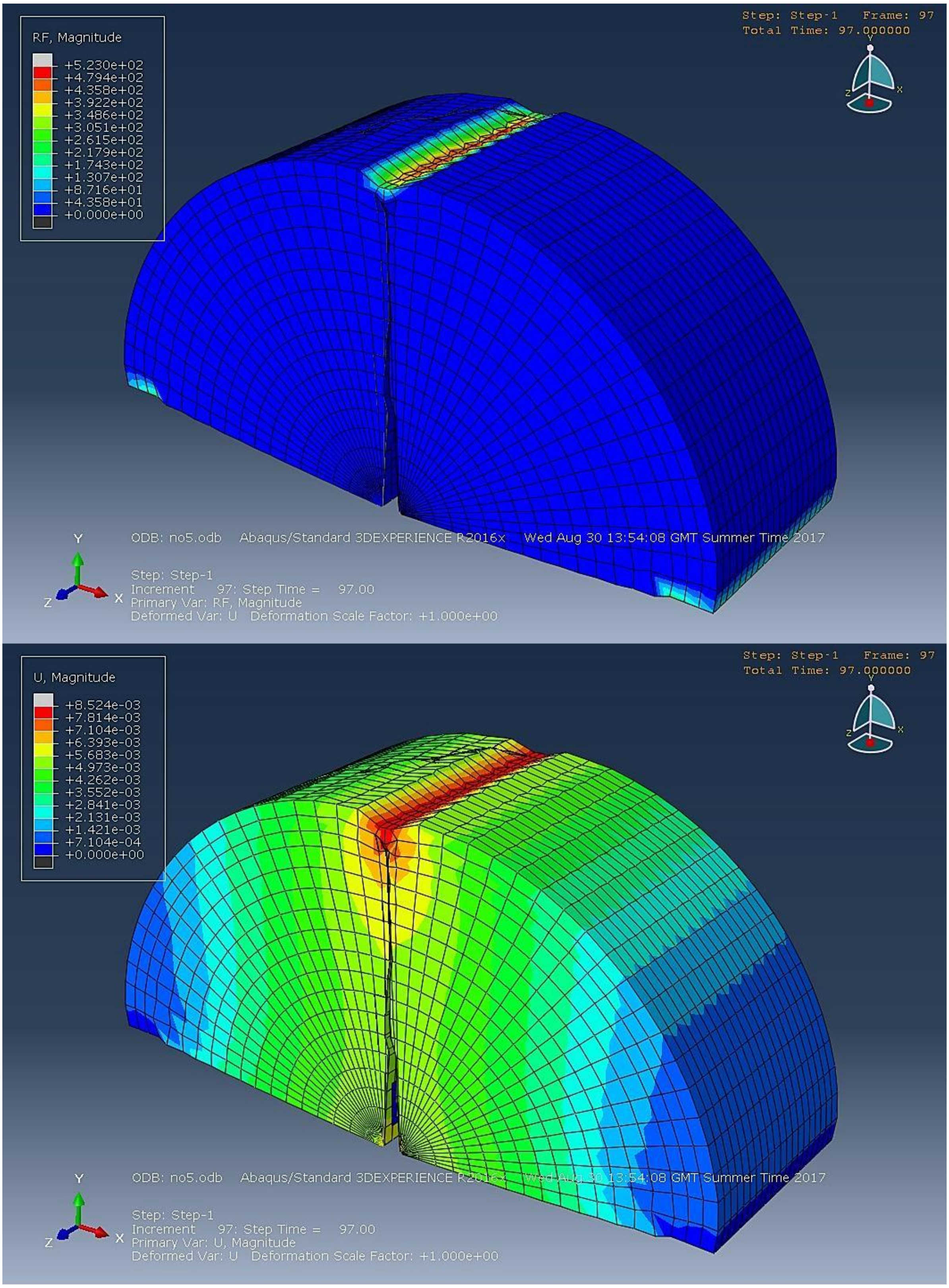

Fig. 14. Level of reaction force and movement of conventional cold mix asphalt model at the second of 97 as a step time

A flow chart revealed the methodology of research in the Figure 15.

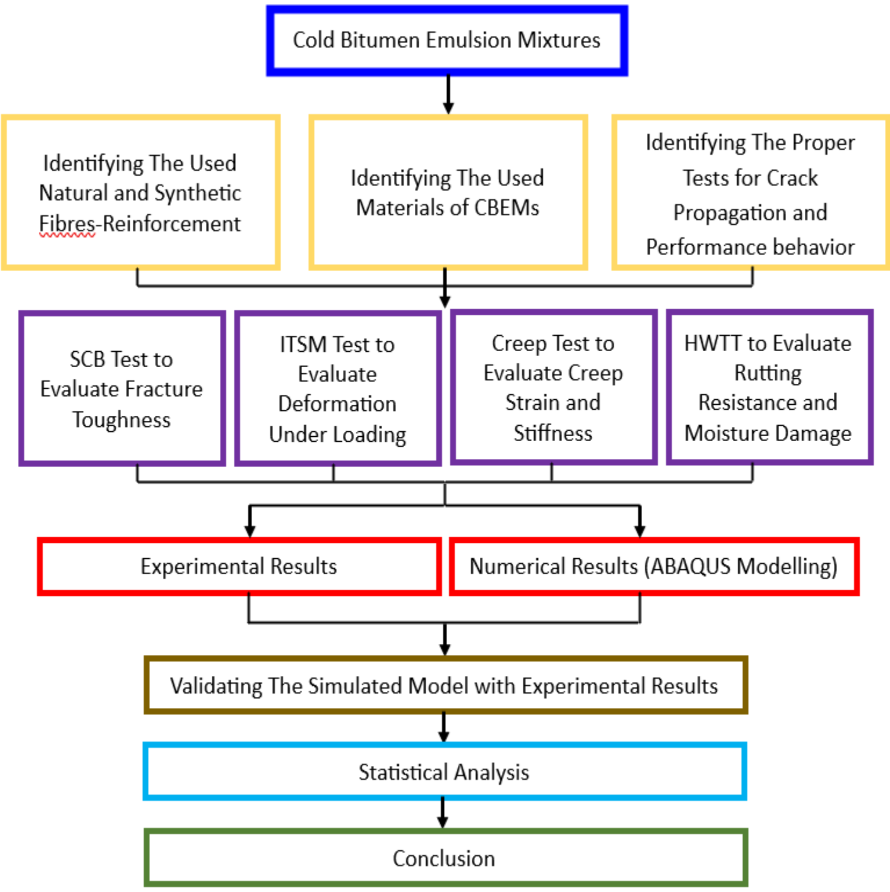

Fig. 15. Approach of research

4. Results and Discussion

4.1 SCB Test Results

This research focuses on evaluating the maximum load capacity of CBEM specimens at failure, as derived from their peak displacement. The corresponding maximum stress is then calculated to conduct the fracture toughness, which is directly related to this stress. Fracture toughness was evaluated using monotonic semi-circular bending (SCB) tests, analyzing the load-displacement behavior across three CBEM types: conventional cold bituminous emulsion mixture, natural reinforcement of CBEM (coir fibre), and synthetic reinforcement CBEM (glass fibre). Among these, glass fibre-reinforced CBEMs achieved the highest fracture toughness and maximum stress due to the high strength, stiffness, and energy absorption capacity of glass fibres, which enhance resistance to crack initiation and propagation. The ultimate stress at failure (σ_{max}) of all cold bituminous emulsion mixtures was calculated using Eq. (3), as described previously and presented in Table (3), below:

Table 3. Failure stress at maximum level (experimentally)

σ_{max} of conventional CBEM	σ_{max} of CBEM modified with coir fibre	σ_{max} of CBEM modified with glass fibre
1.455 (N/mm^2)	2.211 (N/mm^2)	2.688 (N/mm^2)

The results showed that incorporating coir fibre increased the ultimate stress (σ_{max}) by 52%, at the same time glass fibre reinforcement led to increase the ultimate stress by 85% in comparison to conventional CBEM. The enhancement in the ultimate stress of the modified CBEMs with coir fibres is basically owing to natural lignocellulosic composition of these fibres, which contribute in a moderate tensile strength and flexibility. These kinds of fibres aid in bridging the micro-cracks and improving the distribution of stress with CBEMs. Although, such improving process is limited owing to the effects of coir fibres within CBEMs in lowering the stiffness and decreasing the interfacial bonding. Meanwhile, the glass fibres contribute in increasing the ultimate stress due to their effects within CBEMs in rising the levels of tensile strength, stiffness and strengthening the interfacial bonding with the CBEM matrix, allowing for more efficient load transfer and better resistance to crack propagation.

Rasheed A. [28], examine a resistance of cold mix asphalt samples to crack and deformation with as well as without reinforcement of glass fibre to enhance mixture performance in road maintenance. Rasheed A.'s study showed improvements in tensile strength reaching 15% at maximum load failure and 33% at ultimate failure in comparison to control micro asphalt, based on three-point bending tests. However, the current study represents a significant advancement in the field, offering superior mechanical performance and paving the way for future innovations in fibre-reinforced CBEMs, ensuring greater durability, resilience, and environmental sustainability in pavement engineering. Figure (16), shows the load-displacement behavior of CBEMs during SCB tests.

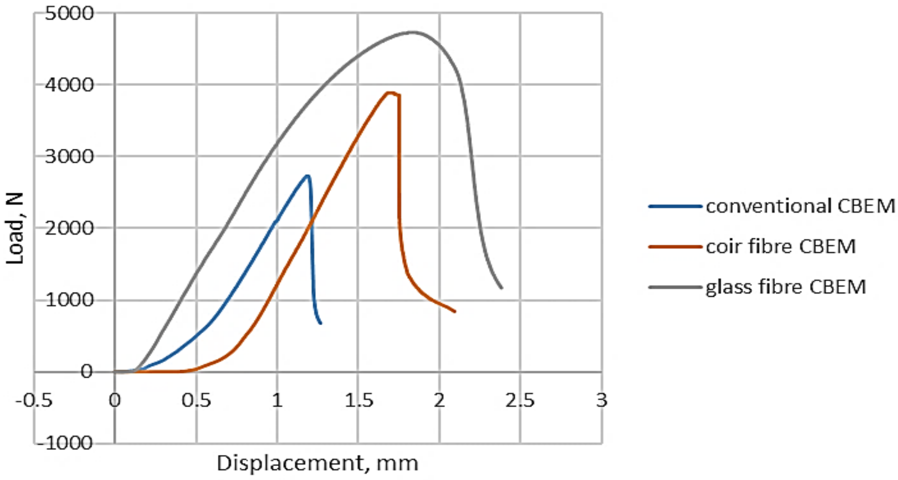

Fig. 16. Load-displacement behavior of CBEMs in SCB tests

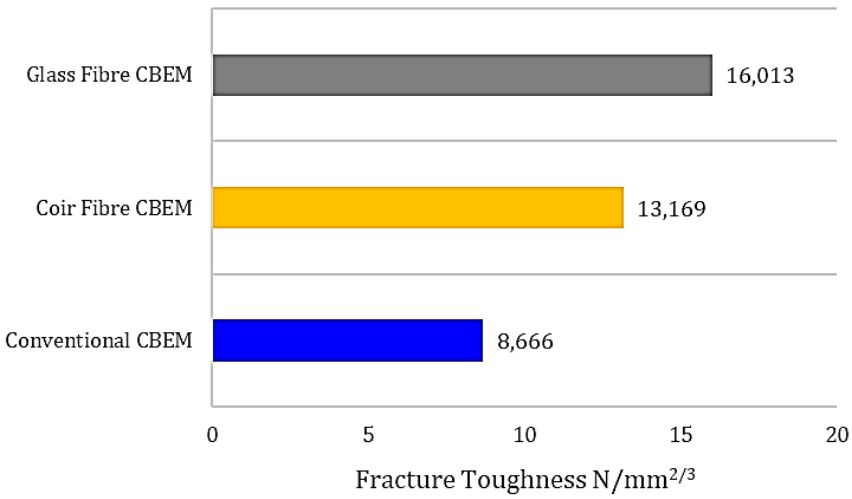

Fig. 17. Fracture toughness of the adopted types of CBEMs

Subsequently, the fracture toughness of the conventional samples of CBEM, as well as the modified CBEM with coir fibre and glass fibre, was calculated based on the concentrated stress obtained from the monotonic semi-circular bending test and by applying Eq. (4), as described previously. The intended toughness of fracture consequences is presented in Figure (17).

The results showed that fracture toughness increased by 52% with coir fibre and by 85% with glass fibre, compared to the conventional CBEM. The adopted glass fibres reveal a superior performance due to their mechanical properties and stronger interaction with the CBEM. The natural and more ductile coir fibres provide a remarkable boost in toughness; however, coir fibres contribute to lower stiffness and exhibit weaker bonding within CBEMs. Zhao S., et al. [29], investigated the fracture properties of cement emulsified asphalt mortar (CEAM), by optimizing the binder and emulsion content in order to enhance the performance. Their achieved result in term of the fracture toughness was 10.0 $N/mm^{2/3}$, which is lower than the conducted results in the current study. On the other hand, the ongoing study has offered new techniques in the field of CBEMs industry by using both natural and synthetic fibers to enhance the mix performance.

4.2 Indirect Tensile Stiffness Modulus (ITSM) Results

The tested fibre reinforced CBEMs in this study showed considerably higher ITSM than conventional CBEMs and most superior performance at 0.4% fibre rate and 15 mm in length. CBEMs reinforced with coir and glass fibres achieved 4400 and 5600 MPa, respectively after 28 days of curing in terms of ITSM, while conventional CBEMs achieved 3000 MPa. This represents an increase of 47% for coir fibres and 87% for glass fibres in comparison with the conventional mix. These improvements are directly related to the particular physical and mechanical properties of each type of fibre:

- Coir fibers are natural lignocellulosic fibers with good tensile strengths but high ductility and superior energy-absorbing ability. Incorporating of these fibres within the matrix of CBEMs leads to form a network that bridges microcracks, delaying their propagation and improving the mixture's resistance to deformation. The nature of their rough surface texture works to enhance the bonding power with the bitumen leading to increase the stiffness of CBEMs. However, these kinds of fibres have common issues related to high absorbent and low stiffness in comparison to synthetic fibres, therefore development process of ITSM remains in moderate level.
- Glass fibers are synthetic fibers with extremely high tensile stress, high stiffness, and chemically stable. Incorporating these fibres within the CBEMs leads to increase the efficiency of load transfer, high resistance to deformation, and creating an internal reinforcing grid to constrains the developed cracks under stress. As a result of thin diameter and strong bonding characteristics of these fibres, it allows stress to be redistributed more effectively, leading to improved ITSM levels. In addition, glass fibres maintain their structural integrity during mixing and curing, resulting in superior mechanical performance.

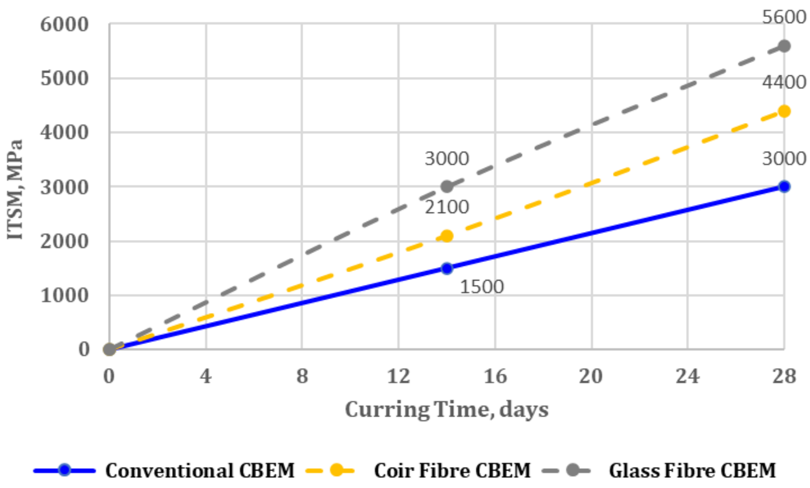

Fig. 18. ITSM Results for Conventional and Reinforced CBEMs

Furthermore, the ITSM of CBEMs increases over time as moisture evaporates and the binder hardens. Initially low due to high water or solvent content, the modulus rises as the mixture gains strength and cohesion, continuing to increase until stabilization. Compared to Du S. [30], who investigated the mechanical performance of cold mix asphalt reinforced with natural and manufactured fibres, including polyester, polypropylene, polyacrylonitrile, lignin, and basalt. The results of the previous study showed improvements in ITSM by 35% with polyester fibres, 30% with polypropylene fibres, 25% with polyacrylonitrile fibres, 20% with lignin fibres, and 30% with basalt fibres. Even though these fibres contributed in the enhancement process of ITSM levels, their improvements were generally lower than those observed with coir and glass fibres in the current study. Figure (18) presents the ITSM results for various CBEMs.

4.3 Creep Test Results

The creep test results at 1000 to 4000 second period, showed that the conventional CBEM, particularly at 60° C, had a consistent rise in strain to 3.0% at 4000s, showing low stiffness and high deformability under heat. Adding coir fibres moderately enhanced the performance by reducing the strain level to 2.0% at 60° C and 1.8% at 40° C after 4000 seconds, showing a little higher stiffness than the conventional CBEMs. The observed improvement in the stiffness due to the influence of coir fibres is attributed to the natural structure of these fibres which provides moderate tensile strength and limits the grown deformation under load. Even though, the irregular surface texture and lower elastic modulus of these fibres contribute in reducing their overall reinforcing efficiency. On the contrary, the glass fibre-reinforced CBEM showed the lowest values of strain (1.2 - 1.3%), which equate to the highest stiffness, showing superior resistance to deformed shape and optimum structural stability at all the temperature regimes and time intervals. The behavior of glass fibres within CBEMs is mainly related to their high tensile strength and stiffness, as well as better interfacial bonding with the CBEM matrix, leading to enhance the load transfer and restrict the development of strain. As a result, the generated CBEMs exhibit lower strain, high stiffness, and better overall structural integrity. Guo Y. et al. [31] examined the effects of different fibre types on the mechanical properties of cold asphalt mixtures and their role in enhancing durability. On the basis of the trends in performance highlighted in their study, the reduction levels of creep strains at 60° C after 4000 seconds of testing was reported as 55% for glass fibers, 45% for polypropylene, 40% for polyester, 30% for basalt, and 20% for cellulose. Comparatively, the ongoing work provides clear and efficient results, with glass fibre-reinforced CBEMs showing a 56.7% improvement in creep resistance, while coir fibre reinforcement resulted in a 33.3% improvement. Consequently, the recent study builds upon previous work by conducting additional performance tests to provide a more comprehensive understanding of fibre reinforcement's impact on CBEM properties. Figure (19) illustrates the creep strain versus time for different CBEMs.

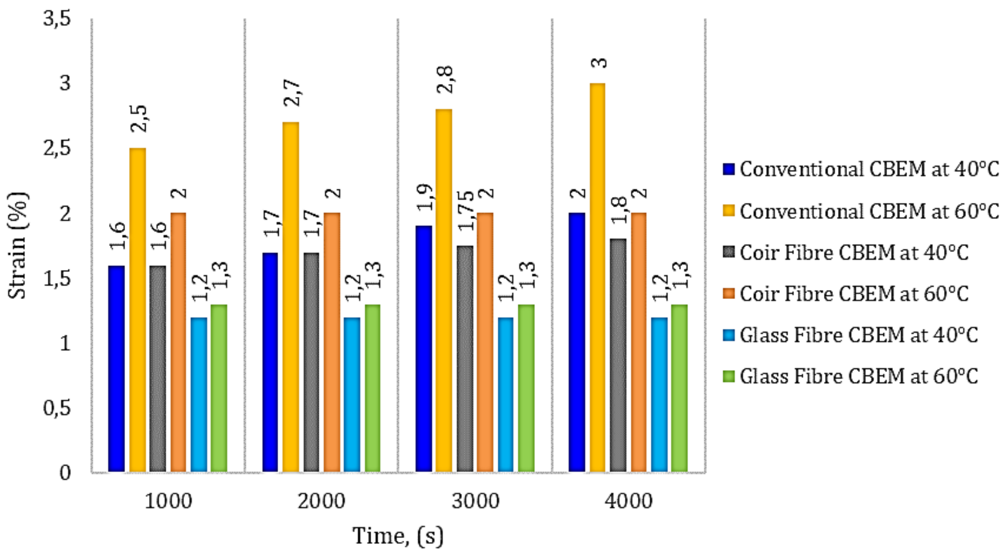

Fig. 19. Creep Strain vs. Time for CBEMs at Different Temperature

4.4 Hamburg Wheel-Track Test Results

The result of Hamburg test revealed an effective improvement in the rutting resistance and moisture sensitivity for both coir and glass modified CEAMs in comparison to conventional mix. After 20000 passes in the wheel-track test, the developed rut depth in the conventional CBEM reached 10.8 mm, indicating poor resistance to permanent deformation and high vulnerability to moisture damage under repeated loading. The incorporation of coir fibres within CBEMs reduced the ruth depth to 6.2 mm, achieving a 43% reduction compared to conventional CBEM. Furthermore, the glass fibre-modified CBEM achieved the lowest rut depth of 4.8 mm, corresponding to a 56% reduction. These improvements are contributed to the ability of the adopted fibres to strengthen the internal matrix of CBEM, effectively control the growth of microcracks, and distribute the applied stresses more efficiently within the mixture. Basically, glass fibers contribute to greater stiffness and tensile strength, strengthening the mixture's structure and improving its rutting and resistance to moisture at advanced stages of loading. Table (4), represent the results of wheel-track test. Amal R et al. [32], investigated the reinforcing process of cold bituminous mixtures using natural coir fibres (20 mm length at 0.25%, 0.5%, and 0.75% by weight of mix). In their study, the optimum fibre dosage (0.5%) resulted in a rut depth of approximately 8.4 mm. On the other hand, the ongoing study demonstrated that coir fibre-modified CBEM achieved a rut depth of 6.2 mm, under the same number of load passes, while glass fibre-modified CBEM exhibited even better performance, with a rut depth of 4.8 mm. Overall, the findings of the current study confirm the superior performance of fibre reinforcement method, specifically with glass fibres, in enhancing rutting resistance and moisture sensitivity under the applied traffic loading.

Table 4. Rut depth for the developed CBEMs (experimentally)

CBEM type / No. of passes	Rut depth in (mm) for the conventional CBEM	Rut depth in (mm) for the coir fibre CBEM	Rut depth in (mm) for the glass fibre CBEM
5000	4.2	2.6	1.8
10000	7.3	4.3	3.1
15000	9.5	5.5	4.2
20000	10.8	6.2	4.8

4.4 Finite Element Modelling (FEM) Results

4.4.1 In Terms of Load-Displacement Behavior

Each cold asphalt mixture specimen exhibited peak force and the corresponding displacement, as shown in Figure (20), which represents the load–displacement of the three CBEM types. CBEMs reinforced with glass and coir fibres outperform conventional CBEMs in terms of load resistance behavior.

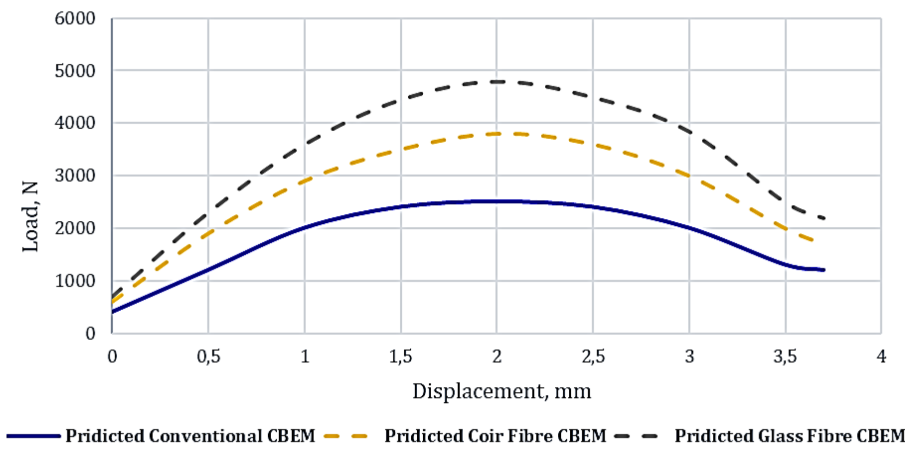

Fig. 20. Load- displacement behavior of cold bituminous emulsion mixture models

The glass fibre-reinforced CBEM achieved the highest load resistance, approximately 4800 N, followed by the coir fibre-reinforced CBEM at around 3750 N, while the conventional CBEM reached 2500 N.

4.4.2 In Terms of Ultimate Stresses at Failure (Stiffness)

The ultimate stress at failure (σ_{max}) of all cold bituminous emulsion mixtures specimens was calculated depending on Eq. (3), as previously described, and the results presented in Table (5), below. As shown in Table (5) above, glass fibre-reinforced CBEM exhibited the highest stiffness, followed by the coir fibre-reinforced CBEM, then the conventional mix.

Table 5. Failure stress at maximum level (modelling)

σ_{max} of conventional CBEM	σ_{max} of CBEM modified with coir fibre	σ_{max} of CBEM modified with glass fibre
1.446 (N/mm^2)	2.129 (N/mm^2)	2.701 (N/mm^2)

4.4.3 In Terms of Fracture Toughness

All three models of cold bituminous emulsion (conventional model, reinforced coir fibre model, and reinforced glass fibre model) were assessed via toughness of fracture (crack growth resistant) based on the determined values of stress demonstrated in Table (5) above, and calculated using Eq. (4), as previously described. Figure (21), shows the fracture toughness of the numerical models of cold mix asphalt specimens.

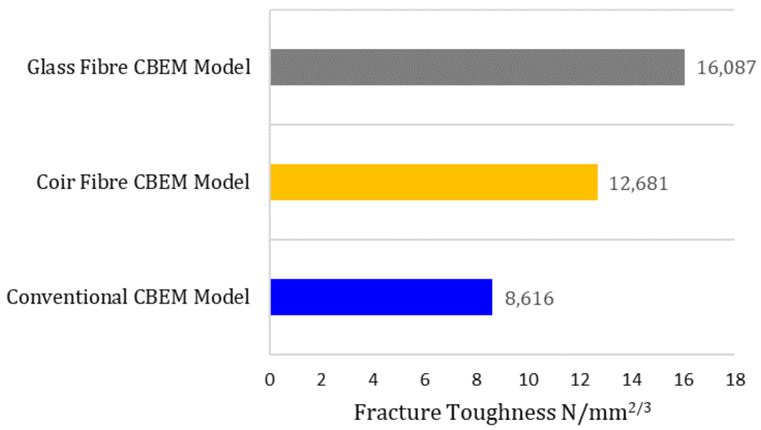

Fig. 21. Fracture toughness of the adopted types of CBEMs models

Figure (21), clearly shows that the glass fibre-reinforced CBEM recorded the highest fracture toughness, followed by the coir fibre-reinforced CBEM. Furthermore, the conventional cold mix asphalt revealed the lowest resistance to crack growth.

4.4.4 In Terms of Performance Behavior

The FEM, conducted through ABAQUS software, successfully simulated the experimental rut behavior, enabling accurate prediction of rut depth progression under repeated loading. The glass fibre-reinforced CBEM exhibited the lowest rut depths, followed by the coir fibre-reinforced CBEM, while the conventional CBEM recorded the highest rut depths, as shown in Table (6), below.

Table 6. Rut depth for the developed CBEMs (modelling)

CBEM type / No. of passes	Rut depth in (mm) for the conventional CBEM	Rut depth in (mm) for the coir fibre CBEM	Rut depth in (mm) for the glass fibre CBEM
5000	4.4	2.7	1.9
10000	7.6	4.5	3.3
15000	9.8	5.8	4.4
20000	11.2	6.5	5.1

4.5 FEM Validation

4.5.1 Comparison Approach

The results of finite element modelling (FEM) closely matched the experimental findings, confirming the model's reliability in simulating crack propagation and performance behavior of CBEMs under loading conditions, as shown in Figures 22 and 23.

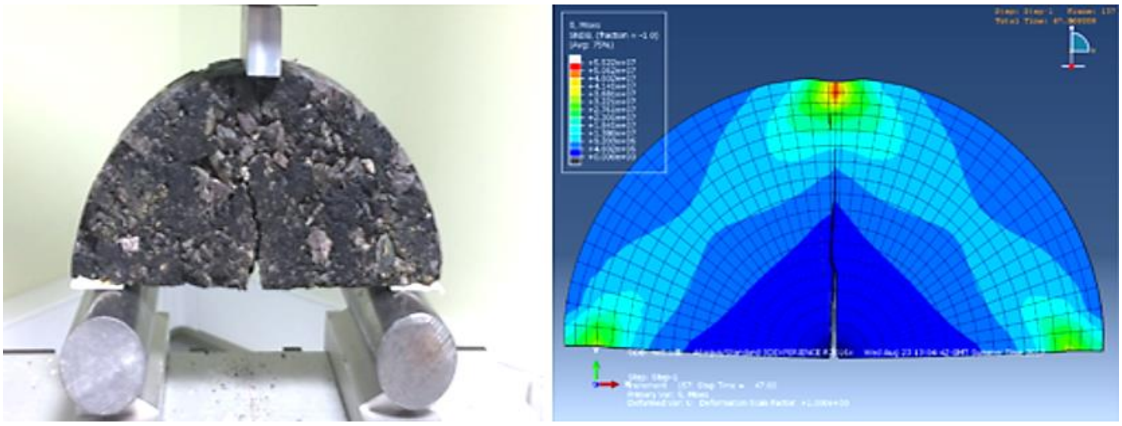

Fig. 22. Validation of experimental and numerical results for crack propagation in CBEM

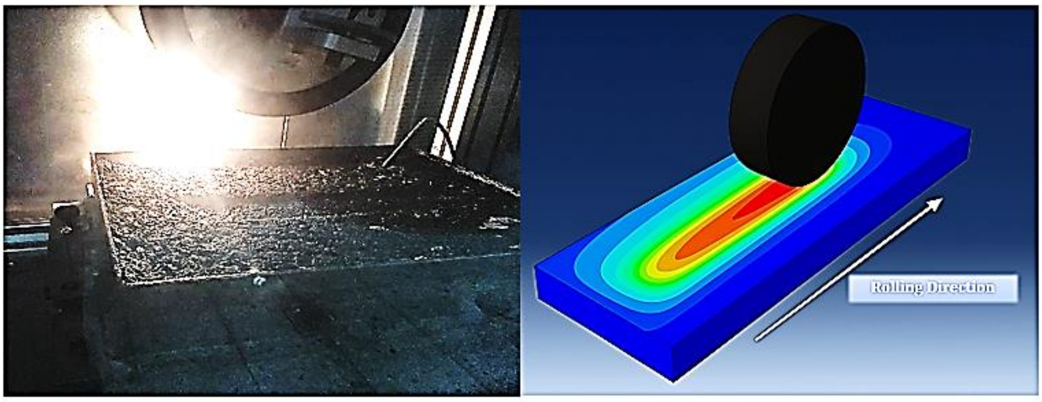

Fig. 23. Validation of experimental and numerical results for performance behavior in CBEM

Figure (24), presents the findings from laboratory SCB tests and FEM simulations for a 10 mm crack notch in conventional CBEM. The FEM accurately replicates the load-displacement curve when compared to the experimental data. Both the experimental and FEMs recorded reaction forces of approximately 2500 N, then the experimental load-displacement curve begins to decline gradually in comparison to FEM curve, approximately at a displacement of 1.3 mm. Figure (25), presents the FEM alongside the laboratory SCB test results for CBEM reinforced with coir fiber. The FEM provides a reasonable estimation in comparison to the experimental data, with both exhibiting similar load-displacement behavior. However, the experimental load-displacement curve begins to decline earlier than the FEM curve, approximately at a displacement of 1.6 mm. The greatest alignment between the load-displacement curves of the FEM and the experimental work is observed in the CBEM reinforced with glass fiber, as illustrated in Figure (26). The figure shows that the maximum load required to reach peak displacement is nearly identical in both the experimental SCB test and the FEM simulation, with a peak load of approximately 4900 N and a displacement of 1.9 mm.

Figure (27), clearly demonstrates that the fracture toughness values from the FEM analysis closely align with those from the experimental SCB tests for all three types of CBEM. The FEM, performed using ABAQUS software, effectively captured the experimental results, enabling accurate prediction of crack growth behavior through both experimental and numerical methods. Figure (28), reveals perfect alignment between the experimental rut depth behavior and the simulated FEM of ABAQUS for all the types of CBEMs, under all the applied wheel-track passes.

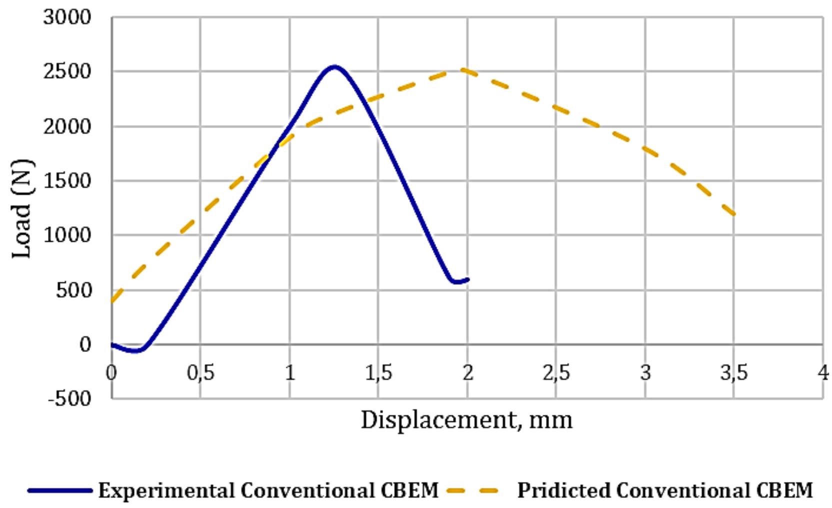

Fig. 24. Comparison of experimental work with FEM load-displacement curves for conventional CBEM

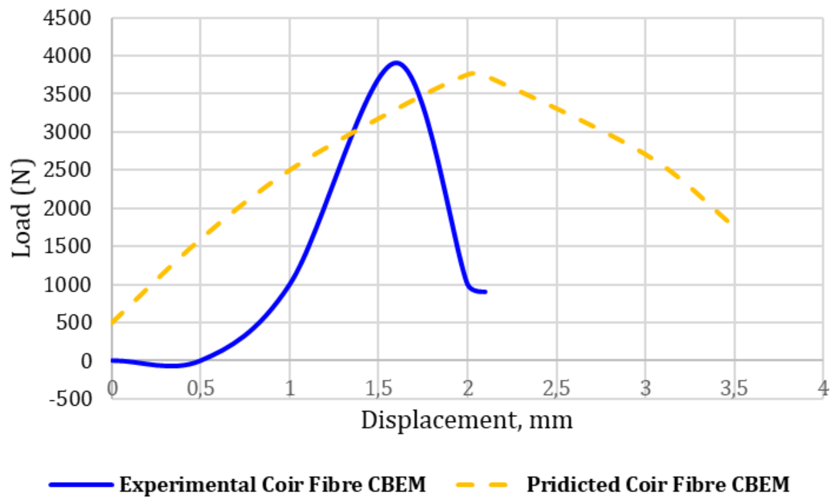

Fig. 25. Comparison of experimental work with FEM load-displacement curves of CBEM reinforced with coir fibre

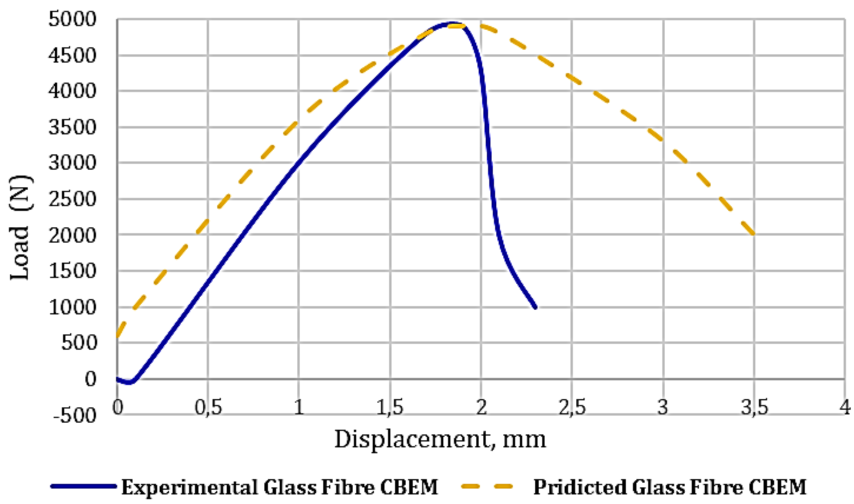

Fig. 26. Comparison of experimental work with FEM load-displacement curves of CBEM reinforced with glass fibre

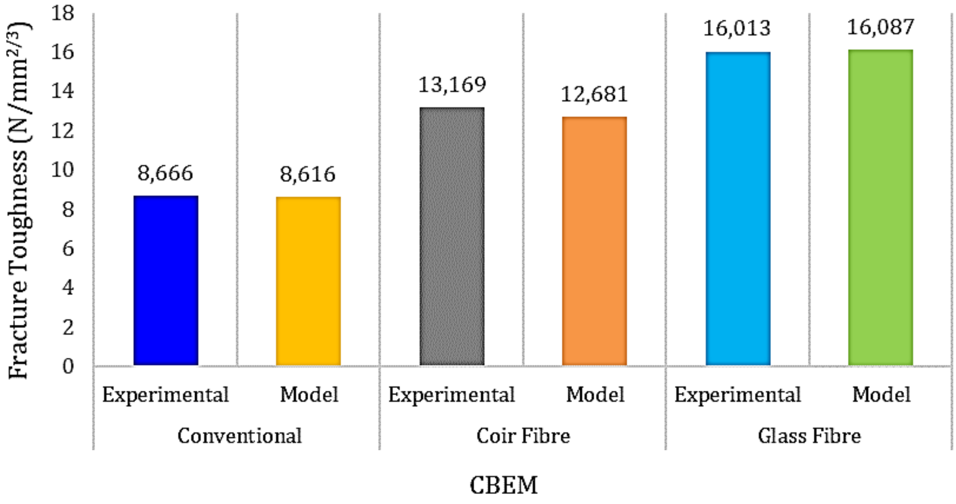

Fig. 27. Fracture toughness results from both the experimental method and the FEM method

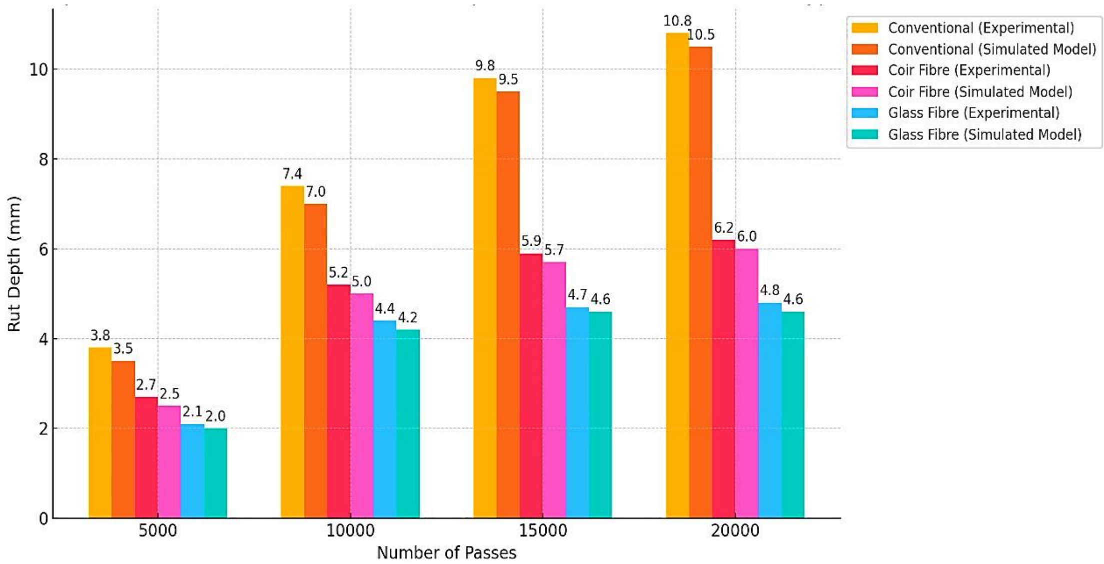

Fig. 28. Experimental vs. simulated FEM rut depth for all the types of CBEMs

4.5.2 Statistical Validation

To support the reliability and credibility of the achieved fracture toughness results for both experimental and numerical data of CBEMs, standard deviation and one-way ANOVA analysis were implemented to confirm the significance of differences between CBEM types, as shown below:

4.5.2.1 Part 1: Standard deviation of differences

The differences between experimental and numerical data for fracture toughness results are concluded from the previous Figure (27), as shown below in Table (7).

Table 7. The difference values between experimental and numerical results of fracture toughness for CBEMs

CBEM type	Fracture toughness experimental values / N/mm$^{2/3}$	Fracture toughness numerical values / N/mm$^{2/3}$	The difference values
Conventional	8.666	8.616	0.050
Coir fibres	13.169	12.681	0.488
Glass fibres	16.013	16.087	-0.074

- 1- Mean of differences (D), as in Eq. (5).

$$D = \frac{0.050 + 0.488 + (-0.074)}{3} = 0.1547 \tag{5}$$

- 2- Squared Deviations from the Mean, as in Eq. (6).

$$\sum (D_i - D)^2 = 0.01097 + 0.1111 + 0.0523 = 0.17437 \tag{6}$$

D_i: The difference between the experimental and numerical data

- 3- Variance (S^2), as is Eq. (7).

$$S^2 = \frac{\sum (D_i - D)^2}{n - 1} = \frac{0.17437}{2} = 0.0872 \tag{7}$$

n: The number of pairs

- 4- Standard Deviation (S), as in Eq. (8).

$$S = \sqrt{S^2} = \sqrt{0.0872} = 0.2953 \tag{8}$$

4.5.2.2 Part 2: One-Way ANOVA

- 1- Grand mean (GM), as in Eq. (9).

$$GM = \frac{8.666 + 13.169 + 16.013 + 8.616 + 12.681 + 16.087}{6} = 12.5387 \tag{9}$$

- 2- Sum of squares between experimental and numerical groups (SSB), as in Eq. (10).

$$\begin{gathered} SSB = n\,(\bar{x_1} - GM)^2 + n\,(\bar{x_2} - GM)^2 \\ SSB = 3 \times (0.0060) + 3 \times (0.0061) = 0.0364 \end{gathered} \tag{10}$$

$\bar{x_1}$: 12.616 (mean of experimental); $\bar{x_2}$: 12.461 (mean of numerical); n: 3 (values per group)

- 3- Sum of squares within experimental and numerical groups (SSW), as in Eq. (11).

$$\begin{gathered} SSW = 27.4519 + 27.9855 = 55.4374 \\ SSW_{Experimental} = (8.666 - 12.616)^2 + (13.169 - 12.616)^2 + (16.013 - 12.616)^2 = 27.4519 \\ SSW_{Numerical} = (8.616 - 12.461)^2 + (12.681 - 12.461)^2 + (16.087 - 12.461)^2 = 27.9855 \end{gathered} \tag{11}$$

- 4- Degrees of freedom (df), as in Eq. (12), and Eq. (13).

$$df_1 = k - 1 = 2 - 1 = 1 \tag{12}$$

$$df_2 = N - k = 6 - 2 = 4 \tag{13}$$

df_1: degree of freedom between experimental and numerical groups; df_2: degree of freedom within experimental and numerical groups; *k:* 2 (number of groups); *N:* 6 (total observations: 3 experimental + 3 numerical)

- 5- Mean squares (MS), as in Eq. (14), and Eq. (15).

$$MS_{between} = \frac{SSB}{df_1} = \frac{0.0364}{1} = 0.0364 \tag{14}$$

$$MS_{within} = \frac{SSW}{df_2} = \frac{55.4374}{4} = 13.8593 \tag{15}$$

- 6- F-statistic, as in Eq. (16).

$$F = \frac{MS_{between}}{MS_{within}} = \frac{0.0364}{13.8593} = 0.0026 \tag{16}$$

- 7- p-Value

$p = 0.9619 \cong 96\%$

The statistical validation conducted using standard deviation and one-way ANOVA confirmed that there is no significant difference between the experimental and numerical fracture toughness values. The low standard deviation (0.2953 $\mathrm{N/mm^{2/3}}$) and high p-value (0.9619) indicate strong agreement, thereby validating the reliability and accuracy of the numerical model in simulating the fracture behavior of the adopted CBEMs.

4.6 STATUSXFEM

XFEM is a scheme available in ABAQUS software was employed to Effectively predict crack propagation in CBEMs. A crucial output variable in XFEM is STATUSXFEM ("status of the enriched element"), which signifies the condition of present cracks. The sample is fully cracked when its STATUSXFEM value reaches 1.0, whereas a STATUSXFEM of 0.0 indicates an entirely intact sample with no cracks. If the STATUSXFEM value falls between 0.0 and 1.0, the element is partially cracked, reflecting progressive damage [33]. As shown in Figure (29), the sample becomes fully fractured when time of step reaches 47 seconds, as indicated by the scheme of extended finite element value reaching 1.0.

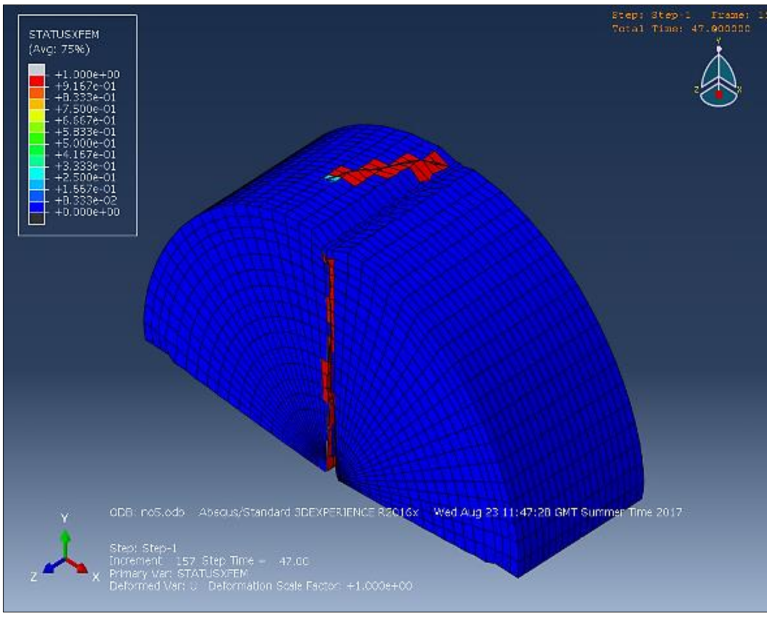

Fig. 29. The extended finite element scheme for three types of cold mix asphalt samples

Fig. 30. Crack length recording under three-point bending test

To conduct a more explicit comparison between the experimental and numerical results, the recorded crack length of the generated CBEMs during the SCB test was employed for this purpose. Here, the test specimen is fixed at the ends with a center load imposed up to the point of failure as shown below in Figure (30). The crack length at a specific time period of 47 second (the same duration of XFEM scheme), was calculated by analyzing crack and fracture behavior during loading though a connected digital dial gauge. The conducted comparison between the experimental and numerical data are illustrated in Table (8), in terms of the generated crack length under loading.

Table 8. CBEMs crack length for both experimental and numerical generated data

CBEM type	Experimental crack length (mm)	XFEM crack length (mm)
Conventional CBEM	1.300	1.235
Coir fibres CBEM	0.855	0.812
Glass fibres CBEM	0.704	0.669

Both experimental and the XFEM numerical results are considerably combined, revealing a strong agreement in crack length predictions at the 47-second time mark. To support this alignment in results, the coefficient of correlation (R^2), mean absolute error (MAE), and root mean squared error (RMSE) are additionally calculated as show below:

- Step 1: Compute the mean of experimental crack lengths (y^{-}), as in Eq. (17).

$$y^{-} = \frac{1.300 + 0.855 + 0.704}{3} = 0.953\ mm \tag{17}$$

- Step 2: Compute the errors

$|\mathrm{y_i} - \mathrm{y_i^{\wedge}}| = 0.065$ for convensional, 0.043 for coir fibres, 0.035 for glass fibres ;

$(\mathrm{y_i} - \mathrm{y_i^{\wedge}})^2 = 0.0042$ for convensional, 0.0018 for coir fibres, 0.0012 for glass fibres

$\mathrm{y_i} - \mathrm{y_i^{\wedge}} = 0.065$ for convensional, 0.043 for coir fibres, 0.035 for glass fibres

yi: Experimental crack length for each CBEM type

yi^: XFEM-predicted crack length for each CBEM type

- Step 3: Calculate the error metrics, as in Eq. (18), Eq. (19), and Eq. (20).

$$Mean\ Absolute\ Error\ MAE = \frac{\sum|y_i - y_i^{\wedge}|}{n} = \frac{0.065 + 0.043 + 0.035}{3} = 0.0477mm \tag{18}$$

$$Root\ Mean\ Squared\ Error\ RMSE = \sqrt{\frac{\sum(y_i - y_i^{\wedge})^2}{n}} = \sqrt{\frac{0.0042 + 0.0018 + 0.0012}{3}} = 0.0493mm \tag{19}$$

$$Coefficient\ of\ Corrilation\ (R^2) = 1 - \frac{\sum(y_i - y_i^{\wedge})^2}{\sum(y_i - y^{-})^2} = 1 - \frac{0.0042 + 0.0018 + 0.0012}{0.1204 + 0.0096 + 0.0620} = 0.962\ \cong 96\% \tag{20}$$

5. Conclusion

Integrating natural and synthetic fibres into CMA effectively enhances its mechanical properties. These fibres strengthen the asphalt matrix, improving resistance to cracking and resulting in greater durability. Natural fibres offer a sustainable, cost-effective option, whereas synthetic fibres provide greater strength and long-term stability. The objective of this research was to carry out in-depth analysis of the semi-circular bending (SCB) test to evaluate the cracking resistance of fibre reinforced cold mix asphalt.

Furthermore, the rutting performance was analyzed by performing the Hamburg wheel-track test (HWTT) to assess the mixtures' resistance to permanent deformation and sensitivity to moisture under repeated traffic. Moreover, a 3D model of finite element was utilized to validate experimental SCB and the wheel- track results, providing a detailed analysis of the failure mechanism, and the mixtures' performance under repeated loading. Besides that, a statistical approach has been employed in terms of fracture toughness and crack length to validate both the experimental and numerical results. The outcomes concluded from this investigation are: -

- The optimal ITSM results are achieved when the fibre is 15 mm in length and the content of fibre is 0.4%.

- Reinforcing the conventional CBEM with coir and glass fibres significantly increased the tensile strength by 47% and 87%, respectively, resulting in notable improvements in the ITSM.
- Employing both coir and glass fibres within CBEMs, led to decrease the creep strain by 33.3% and 56.7%, respectively, compared to the conventional mix at 60° C after 4000 seconds of testing. Likewise, at 40° C and after 4000 seconds, the creep strain decreased by 10% and 66.7%, respectively, in comparison to conventional mix.
- Incorporating both coir and glass fibres within CBEMs led to a substantial increase in creep stiffness compared to the conventional CBEM, across different temperatures.
- Integrating both both coir and glass fibres within CBEMs led to increase the fracture toughness by 52% and 85%, respectively, compared to the conventional CBEM, revealing a superior performance of glass fibres.
- Utilizing both coir and glass fibres within CBEMs led to decrease the rutting depth by 43% and 56%, respectively, in comparison to conventional CBEM. This demonstrates the effectiveness of using such fibres to enhance CBEM performance in terms of rutting resistance and moisture susceptibility.
- The conducted FEMs in terms of load-displacement behavior, ultimate stresses at failure (stiffness), fracture toughness, and performance behavior under repeated loading, achieved considerable alignment with the experimental results, confirming the model's reliability and efficiency.
- The adopted statistical approach in terms of fracture toughness confirmed that there was no significant difference between the experimental and numerical values, thereby validating the reliability and accuracy of the numerical model in simulating the fracture behavior of the adopted CBEMs.
- The used statistical analysis between the experimental and the XFEM numerical results revealed a strong agreement in crack length predictions, achieving a coefficient of correlation (R^2) of 96%.

This study has purposes of investigating the impact of natural and synthetic fibres on the crack resistance of CMA, tensile strength of CMA, strain resistance, rutting resistance, and to simulate these effects using FEA with ABAQUS. However, a key limitation of this research is the absence of additional service tests, for example the long-term durability testing, aging effects, and the test of asphalt pavement analyzer (APA) for assessing fatigue cracking. In addition, a detailed cost–benefit and lifecycle assessment for the developed CBEMs is acknowledged as one of the study's limitations. To enhance this research, future studies should focus on addressing these limitations.

References

[1] Rogo KU. Performance of fine dense-graded cold mix asphalt incorporating spent garnet and palm oil fuel ash (Doctoral dissertation, Universiti Teknologi Malaysia).
[2] Kim C, Lawson K, Rajan J, Tan A. 2020 CBEMS Design Project.
[3] Deb P, Lakshman Singh K. Mix design, durability and strength enhancement of cold mix asphalt: a state-of-the-art review. Innovative Infrastructure Solutions. 2022 Feb;7:1-22. https://doi.org/10.1007/s41062-021-00600-2
[4] Gunarathne DS, Udugama IA, Jayawardena S, Gernaey KV, Mansouri SS, Narayana M. Resource recovery from bio-based production processes in developing Asia. Sustainable Production and Consumption. 2019 Jan 1;17:196-214. https://doi.org/10.1016/j.spc.2018.11.008
[5] Safazadeh F, Romero P, Mohammad Asib AS, VanFrank K. Methods to evaluate intermediate temperature properties of asphalt mixtures by the semi-circular bending (SCB) test. Road Materials and Pavement Design. 2022 Jul 3;23(7):1694-706. https://doi.org/10.1080/14680629.2021.1911831
[6] Liu Z, Gu X, Ren H, Zhou Z, Wang X, Tang S. Analysis of the dynamic responses of asphalt pavement based on full-scale accelerated testing and finite element simulation. Construction and Building Materials. 2022 Mar 28;325:126429. https://doi.org/10.1016/j.conbuildmat.2022.126429
[7] Sedmak A. Fatigue crack growth simulation by extended finite element method: A review of case studies. Fatigue & Fracture of Engineering Materials & Structures. 2024 Jun;47(6):1819-55. https://doi.org/10.1111/ffe.14277

[8] Wu S, Haji A, Adkins I. State of art review on the incorporation of fibres in asphalt pavements. Road Materials and Pavement Design. 2023 Jun 3;24(6):1559-94. https://doi.org/10.1080/14680629.2022.2092022
[9] Solak H, İskender E, Aksoy A, İskender C. Use of Synthetic Fibers in Asphalt Pavements-Mini Review. InInternational Conference on Advances in Civil Engineering 2023 Sep 6 (pp. 415-423). Singapore: Springer Nature Singapore. https://doi.org/10.1007/978-981-97-1781-1_38
[10] Addae DT, Rahman M, Abed A. State of art literature review on the mechanical, functional and long-term performance of cold mix asphalt mixtures. Construction and Building Materials. 2023 Oct 12;400:132759. https://doi.org/10.1016/j.conbuildmat.2023.132759
[11] Jain S, Singh B. Cold mix asphalt: An overview. Journal of cleaner production. 2021 Jan 20;280:124378. https://doi.org/10.1016/j.jclepro.2020.124378
[12] Guo Q, Wang H, Gao Y, Jiao Y, Liu F, Dong Z. Investigation of the low-temperature properties and cracking resistance of fiber-reinforced asphalt concrete using the DIC technique. Engineering Fracture Mechanics. 2020 Apr 15;229:106951. https://doi.org/10.1016/j.engfracmech.2020.106951
[13] Li Z, Zhang X, Fa C, Zhang Y, Xiong J, Chen H. Investigation on characteristics and properties of bagasse fibers: Performances of asphalt mixtures with bagasse fibers. Construction and Building Materials. 2020 Jul 10;248:118648. https://doi.org/10.1016/j.conbuildmat.2020.118648
[14] Malik MI, Mir MS, Mohanty B. Cold Bitumen Emulsion Mixtures with Waste Glass: A Laboratory-Driven Investigation into Performance. Journal of Materials in Civil Engineering. 2025 Jan 1;37(1):04024438. https://doi.org/10.1061/JMCEE7.MTENG-17875
[15] Briceño-Balza JE, Castillo-Pernía LJ, Mercado-Marquez M. Evaluation of indirect tensile strength and stability of fiber-reinforced cold asphalt mixes. Revista Ciencia e Ingeniería. Vol. 2025 Dec;46(1).
[16] Jones MR, Halliday JE, Csetenyi L, Zheng L, Strompinis N. Utilising fine and coarse recycled aggregates from the Gulf Region in concrete. InProceedings of the TMS Middle East-Mediterranean Materials Congress on Energy and Infrastructure Systems (MEMA 2015) 2016 (pp. 13-23). Springer International Publishing. https://doi.org/10.1002/9781119090427.ch2
[17] Naamandadin NA, Rosdi MS, Mustafa WA, Aman MN, Saidi SA. Mechanical behaviour on concrete of coconut coir fiber as additive. InIOP Conference Series: Materials Science and Engineering 2020; 932(1): 012098). IOP Publishing. https://doi.org/10.1088/1757-899X/932/1/012098
[18] Kamath SS, Chandrappa RK. Additives used in natural fibre reinforced polymer composites-a review. Materials Today: Proceedings. 2022 Jan 1;50:1417-24. https://doi.org/10.1016/j.matpr.2021.08.331
[19] Zhang Y, Sun L, Cheng H. Effects of nominal maximum aggregate size and compaction effort on the mechanical properties of hot-mix asphalt (HMA). Construction and Building Materials. 2022 Mar 21;324:126715. https://doi.org/10.1016/j.conbuildmat.2022.126715
[20] Shubbar A, Nasr MS, Kadhim A, Hashim TM, Sadique M. Performance Comparison of 45° and 90° Herringboned Permeable Interlocking Concrete Pavement. Infrastructures. 2023 May 22;8(5):97. https://doi.org/10.3390/infrastructures8050097
[21] Al-Jumaili MA, Issmael OD. Sustainability of Cold Recycled Mixture with High Reclaimed Asphalt Pavement Percentages. Appl. Res. J. 2016;2:344-52.
[22] Wright M, James D, Sanchez D, Wayman M, D'Angelo G, Parajuli U, Airey G, Hadley A, Brough C. Laboratory Evaluation of the Performance of Bio-Binders in Conjunction with WMA & RA. InThe International Workshop on the Use of Biomaterials in Pavements 2024 Sep 20 (pp. 24-34). Cham: Springer Nature Switzerland. https://doi.org/10.1007/978-3-031-72134-2_3
[23] Meng Y, Kong W, Gou C, Deng S, Hu Y, Chen J, Fan L. A review on evaluation of crack resistance of asphalt mixture by semi-circular bending test. Journal of Road Engineering. 2023 Mar 1;3(1):87-97. https://doi.org/10.1016/j.jreng.2022.07.003
[24] Aljuboryl A, Airey GD, Grenfell JR. Laboratory evaluation of stiffness and fatigue susceptibility of asphalt paving materials incorporating environmental factors. InBearing capacity of roads, railways and airfields 2017 Jul 20 (pp. 223-230). CRC Press. https://doi.org/10.1201/9781315100333-29
[25] Hashim TM, Abbas GH, Al-Khafaji FF, Alwash AA, Al-Mulali MZ, Ali YA. Using papyrus fiber ash as a sustainable filler modifier in preparing low moisture sensitivity HMA mixtures. Journal of the Mechanical Behavior of Materials. 2022 Aug 29;31(1):649-55. https://doi.org/10.1515/jmbm-2022-0072
[26] Wasilewska M, Grzyb D, Gardziejczyk W. Preliminary assessment of the properties of composite layers based on porous asphalt and coloured mortar. InMATEC Web of Conferences 2024 (Vol. 396, p. 02005). EDP Sciences. https://doi.org/10.1051/matecconf/202439602005
[27] Sukumar N, Moës N, Moran B, Belytschko T. Extended finite element method for three-dimensional crack modelling. International journal for numerical methods in engineering. 2000 Aug 20;48(11):1549-70. https://doi.org/10.1002/1097-0207(20000820)48:11<1549::AID-NME955>3.0.CO;2-A
[28] Rasheed A. Development of a New Environmentally Friendly Glass Fibre Reinforced Cold Mix Microasphalt with High Resistance to Cracking and Deformation. Liverpool John Moores University (United Kingdom); 2018.

[29] Zhao S, Ouyang J, Yang W. Research on fracture properties of cement emulsified asphalt mortar based on viscoelastic fracture mechanics. Construction and Building Materials. 2025 Apr 4;470:140664. https://doi.org/10.1016/j.conbuildmat.2025.140664

[30] Du S. Effect of different fibres on the performance properties of cold recycled mixture with asphalt emulsion. International Journal of Pavement Engineering. 2022 Aug 24;23(10):3444-53. https://doi.org/10.1080/10298436.2021.1901100

[31] Guo Y, Tataranni P, Sangiorgi C. The use of fibres in asphalt mixtures: A state of the art review. Construction and Building Materials. 2023 Aug 1;390:131754. https://doi.org/10.1016/j.conbuildmat.2023.131754

[32] Amal R, Narendra J, Sivakumar M, Anjaneyulu MV. Performance Evaluation of Cold Bituminous Mix Reinforced with Coir Fibre. AIJR Proceedings. 2021 Apr 11:559-68. https://doi.org/10.21467/proceedings.112.67

[33] Liu Z, Zhang Y, Liu H, Liu X, Liang J, Shao Z. Fatigue Characteristics Analysis of Carbon Fiber Laminates with Multiple Initial Cracks. Applied Sciences. 2024 Sep 23;14(18):8572. https://doi.org/10.3390/app14188572